

NJC

Accepted Manuscript



This is an *Accepted Manuscript*, which has been through the Royal Society of Chemistry peer review process and has been accepted for publication.

Accepted Manuscripts are published online shortly after acceptance, before technical editing, formatting and proof reading. Using this free service, authors can make their results available to the community, in citable form, before we publish the edited article. We will replace this *Accepted Manuscript* with the edited and formatted *Advance Article* as soon as it is available.

You can find more information about *Accepted Manuscripts* in the [Information for Authors](#).

Please note that technical editing may introduce minor changes to the text and/or graphics, which may alter content. The journal's standard [Terms & Conditions](#) and the [Ethical guidelines](#) still apply. In no event shall the Royal Society of Chemistry be held responsible for any errors or omissions in this *Accepted Manuscript* or any consequences arising from the use of any information it contains.

In situ solvent and counteranion-induced synthesis, structural characterization and photoluminescence properties of Pb-based MOFs

Qi-Bing Bo,* Juan-Juan Pang, Hong-Yan Wang, Chun-Hua Fan and Zhen-Wei Zhang

Abstract: Based on an attempt to investigate the influence of solvent and counteranion on the structures and photoluminescent properties of Pb-based metal-organic frameworks, the hydrothermal reactions of the same amounts of $\text{Pb}(\text{NO}_3)_2$ and $\text{Pb}(\text{OAc})_2$ with the ligand 5-tert-butylisophthalic acid (H_2tip) in the presence of water and water/ethanol mixture have yielded three compounds $[\text{Pb}(\text{H}_2\text{O})(\text{tip})]_n$ (**1**), $[\text{Pb}_3(\mu_4\text{-O})(\text{tip})_2]_n$ (**2**) and $[\text{Pb}_4(\mu_4\text{-O})(\text{tip})_3]_n$ (**3**) under the similar reaction conditions (tip = 5-tert-butylisophthalate anion). These compounds represented the first examples of Pb(II) metal-organic frameworks with H_2tip . All of them have been characterized by means of FT-IR spectra, elemental analysis, single-crystal X-ray diffraction, powder X-ray diffraction, thermogravimetric analysis, and photoluminescence spectra. The reaction processes revealed that **1** and **2** had selectivity for specific solvents. And the selectivity for specific counteranions was also found in **2** and **3**. Single-crystal X-ray diffraction showed that **1** and **3** crystallized in the orthorhombic crystal system with space groups of *Iba2* and *Pna2₁*, respectively, while **2** crystallized in the monoclinic *P2₁/c* space group. The structure of **1** featured a 2D bilayer structure containing a uninodal **sql**-type topological motif with a Schläfli symbol of (4^4) . The 2D layer framework of **2** was constructed from a unique 8-connected hexanuclear cluster secondary building unit $\text{Pb}_6\text{O}_2(\text{COO})_8$, resulting in a uninodal **hxl**-type topological motif with a Schläfli symbol of $(3^6.4^6.5^3)$. The structure of **3** could be described as a 3D microporous framework with a 6-connected tetranuclear cluster $\text{Pb}_4\text{O}(\text{COO})_6$. Topology analysis revealed that **3** represented a uninodal **dia**-type topological motif with a Schläfli symbol of (6^6) . All of the solid state compounds exhibited the photoluminescent properties at room temperature. Furthermore, taking the emissions of the free ligand into consideration, the emissions **1** and **2** could be assigned to metal-centered $s \rightarrow p$ transition transitions, while the emissions of **3** were due to ligand-to-metal charge transfers

*To whom correspondence should be addressed. E-mail: chm_boqb@ujn.edu.cn

School of Chemistry and Chemical Engineering, University of Jinan, Jinan 250022 (China)

† Electronic supplementary information (ESI) available: topological framework, X-ray crystallographic data in CIF format, the experimental and simulated PXRD patterns, FT-IR spectra, TG curves, etc. See DOI:

between the delocalized p bonds of carboxylate groups and p orbitals of Pb(II) centers. Especially, in situ solvent and counteranion-induced synthesis strategy reported here, could afforded us new opportunities for the rapidly designing new materials with interesting structures and properties.

Introduction

The design and construction of functional metal-organic frameworks (MOFs) was one of the most active areas of materials research. The increasingly great interest in these materials was not only due to their intriguing variety of structural topologies but also their promising properties.¹ To date, many MOFs based on d-transition metals, f-lanthanide metals and 3d-4f heterometals have been extensively synthesized and investigated. However, less attention has been paid to the construction of the heavy p-block Pb(II) MOFs.² As a heavy p-block Pb(II) ion, its toxic effects have increased with its increasing use in industry, such as in paints and batteries. As a result, Pb(II) ion polluted the environment and had damaging effects on human health.³ Therefore, a good knowledge of the Pb(II) ion properties, including aspects such as large ion radius, the lone pair of electrons, flexible coordination environment, and variable stereochemical activity, was of great significance to further understand the toxicological properties of Pb(II) ions. Furthermore, it also provided unique opportunities for the construction of Pb-based MOFs with intriguing structural topologies and interesting properties. For the above-mentioned reasons, several types of Pb-based MOFs with organic ligands have been reported.²

In our attempt to investigate the design and control of the self-assembly of d¹⁰- and f-based MOFs with organic ligands, we recently reported that the reaction of the Zn²⁺, Cd²⁺ and lanthanide salts with 5-methylisophthalic acid (H₂mip) and 5-tert-butylisophthalic acid (H₂tip) gave rise to the formation of various luminescent MOFs with novel structures.⁴ As part of our ongoing studies into the development of the coordination chemistry of the heavy main group elements, we chose typical Pb(II) centers with distinct coordination preferences to assemble with the H₂tip ligand. To the best of our knowledge, no work for Pb(II)-tip MOFs has been presented though several other Pb(II) MOFs have been reported and studied by other groups. On the other hand, solvent-induced synthesis of new MOFs has been of particular interest in material chemistry.⁵ In this study, with solvent or counteranion as the only variable, hydrothermal reactions with the same amounts of H₂tip, NaOH, Pb(OAc)₂·3H₂O or Pb(NO₃)₂, yielded to three new Pb-based MOFs [Pb(H₂O)(tip)]_n (**1**), [Pb₃(μ₄-O)(tip)₂]_n (**2**) and [Pb₄(μ₄-O)(tip)₃]_n (**3**) under the same reaction conditions. All of these

MOFs were characterized by single-crystal X-ray diffraction, infrared spectroscopy, thermogravimetric analysis, elemental analysis, PXRD measurements. The solvent and counteranion-induced synthesis and the photoluminescent properties of the products were also discussed in detail.

Results and Discussion

Considering the solvent or counteranion as the only variable component, hydrothermal reactions of 5-tert-butyl isophthalic acid with the same amounts of H_2tip , NaOH , $\text{Pb}(\text{OAc})_2 \cdot 3\text{H}_2\text{O}$ or $\text{Pb}(\text{NO}_3)_2$ afforded three colorless crystals formulated by single-crystal X-ray diffraction as $[\text{Pb}(\text{H}_2\text{O})(\text{tip})]_n$ (**1**), $[\text{Pb}_3(\mu_4\text{-O})(\text{tip})_2]_n$ (**2**) and $[\text{Pb}_4(\mu_4\text{-O})(\text{tip})_3]_n$ (**3**). Where, tip denoted the 5-tert-butylisophthalate dianions. The results of single-crystal X-ray diffraction analysis showed that all of the crystals have different structures, and all the 5-tert-butyl isophthalic acids were deprotonated to coordinate with the Pb^{2+} ions.

Crystal structure of $[\text{Pb}(\text{H}_2\text{O})(\text{tip})]_n$ (**1**):

Single-crystal X-ray diffraction analysis revealed that **1** crystallized in the space group *Iba2* of the orthorhombic crystal system. Figure 1 (represented in “Ball-and-stick” model) showed that the independent crystallographic unit of **1** contained one Pb^{2+} ion, one coordinated water molecule and one tip anion.

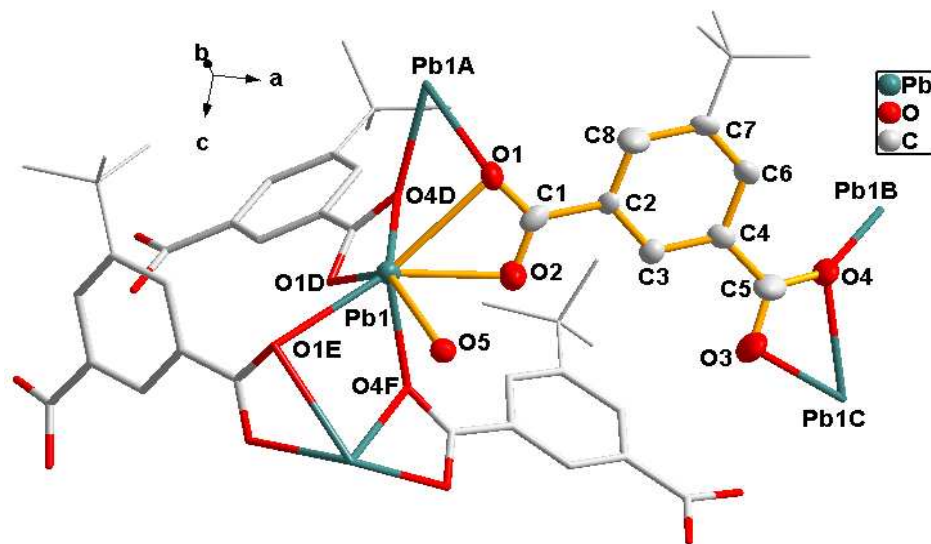
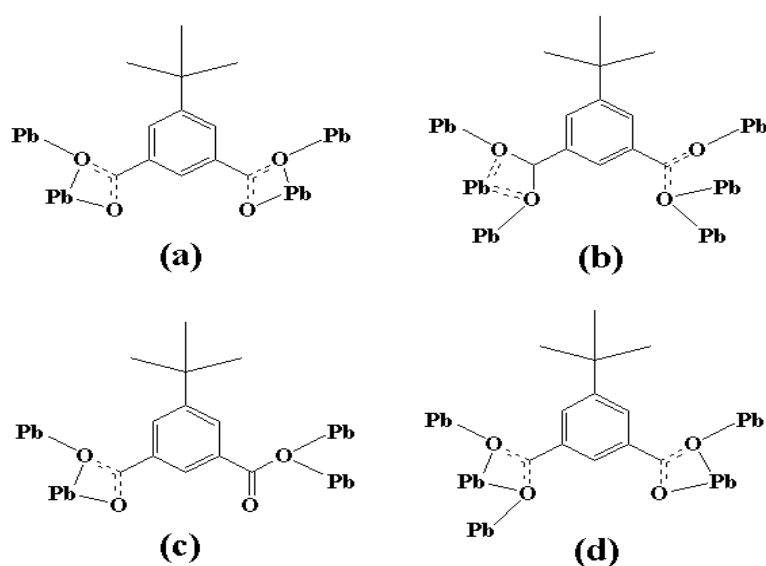


Figure 1 The coordination geometry of the tip ligand and Pb atoms in **1**. Hydrogen atoms are omitted for clarity. symmetry codes: A (-x, y, -0.5+z), B (0.5-x, 1.5-y, -0.5+z), C (0.5+x, 1.5-y, z), D (-0.5+x, 1.5-y, z), E (-x, y, 0.5+z), F (0.5-x, 1.5-y, 0.5+z)

Each Pb center was connected to six carboxylate oxygen donors (O1, O2, O1D, O4D, O1E, O4F) from four different tip anions (Pb-O 2.384-2.817 Å). It is noticeable that the Pb1-O5 distance from the coordinated water molecule (Pb-O 2.938 Å) suggested a nonnegligible interaction,⁶ generating a seven coordination sphere for the lead atom. The coordination environment of tip for **1** revealed that each tip anion acting as bridge-linking ligand coordinated to four adjacent Pb atoms simultaneously with carboxylate groups. And each carboxylate group of tip adopted $\mu_2\text{-}\eta^2\text{:}\eta^1$ -bridging modes (Chart 1a), forming a 2D bilayer structure (labeled with mauve and green parts in Figure 2) in *ac* plane.

Chart 1 Diverse coordination modes of the tip ligands



For each carboxylate group : $\mu_2\text{-}\eta^2\text{:}\eta^1$ -bridging mode (a); $\mu_3\text{-}\eta^2\text{:}\eta^2$ -bis-bridging mode and $\mu_3\text{-}\eta^1\text{:}\eta^2$ -tri-monodentate mode (b); $\mu_2\text{-}\eta^1\text{:}\eta^2$ -bridging mode and $\mu_2\text{-}\eta^0\text{:}\eta^2$ -bis-monodentate mode (c); $\mu_3\text{-}\eta^2\text{:}\eta^2$ -bis-bridging mode and $\mu_2\text{-}\eta^1\text{:}\eta^2$ -bridging mode (d)

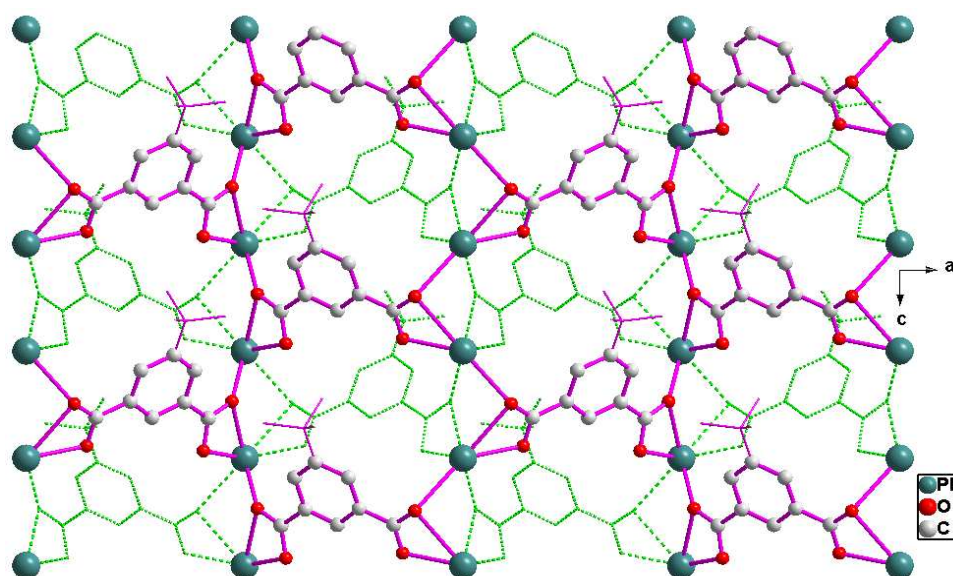


Figure 2 The 2D bilayer structure in *ac* plane for **1**

Considering the tip ligand and the Pb center as nodes, the equivalent 2D topology framework for **1** could be viewed as a uninodal **sql**-type topological motif with a Schläfli symbol of (4^4) , as shown in Supporting Information ESI 1.

Crystal structure of $[\text{Pb}_3(\mu_4\text{-O})(\text{tip})_2]_n$ (**2**):

Single crystal X-ray diffraction analysis indicated that **2** crystallized in the monoclinic crystal system with the space group $P2_1/c$. Figure 3 showed that three Pb^{2+} ions were clustered by tip anions in multiple coordination modes and these three Pb^{2+} ions adopted six, five, and five coordination numbers, respectively.

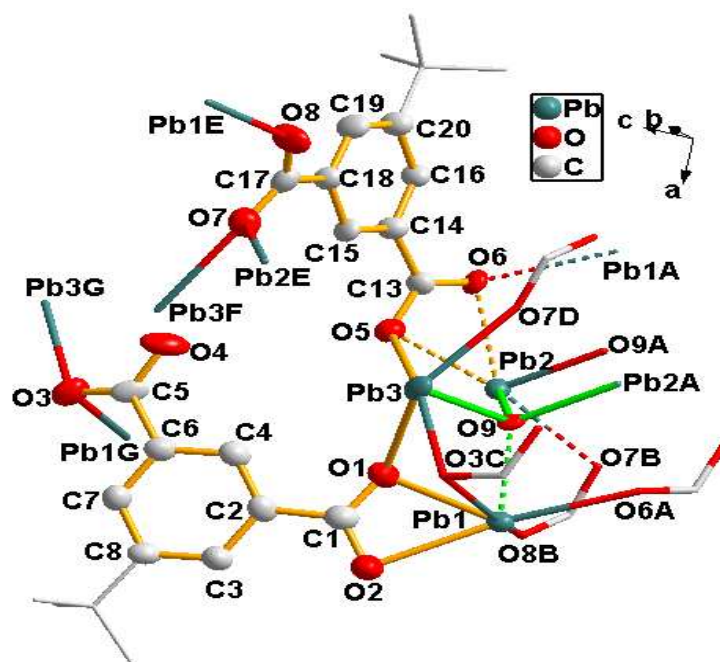


Figure 3 The coordination geometry of the tip ligand and Pb atoms in **2**. Hydrogen atoms are omitted for clarity. symmetry codes: A (-x, 1-y, -z), B (-x, -0.5+y, 0.5-z), C (x, y, -1+z), D (x, 1.5-y, -0.5+z), E (-x, 0.5+y, 0.5-z), F (x, 1.5-y, 0.5+z), G (x, y, 1+z)

The coordination environment of Pb1 was six-coordinated geometry completed by one oxygen atom (O9) from $\mu_4\text{-O}^{2-}$, five carboxylate oxygen atoms (O1, O2, O8B, O6A, O3C) from four tip ligands. Pb2 adopted a five-coordination geometry defined by two oxygen atoms (O9, O9A) from $\mu_4\text{-O}^{2-}$, and three carboxylate oxygen atoms (O5, O6, O7B) from two tip ligands. Pb3 was five-coordinated by one oxygen atom (O9) from $\mu_4\text{-O}^{2-}$ and four carboxylate oxygen atoms (O1, O5, O3C, O7D) from four tip anions. The Pb-O bond lengths were in the range of 2.274-2.802 Å, which were comparable to those reported for other lead(II) carboxylates.⁷ The coordination environment of tip for **2** was shown in Chart 1b and Chart 1c. It is evident that two kinds of the tip anions acting as bridge-linking ligands coordinated to the adjacent lead atoms with carboxylate groups. One adopted $\mu_3\text{-}\eta^2\text{:}\eta^2\text{-bis-bridging}$ mode and $\mu_3\text{-}\eta^1\text{:}\eta^2\text{-tri-monodentate}$ mode (Chart 1b), the other linked the lead atoms adopting $\mu_2\text{-}\eta^1\text{:}\eta^2\text{-bridging}$ mode and $\mu_2\text{-}\eta^0\text{:}\eta^2\text{-bis-monodentate}$ mode (Chart 1c).

It is noteworthy that compound **2** displayed a two-dimensional network consisting of $\mu_4\text{-O}^{2-}$ anion-bridged Pb_6O_2 clusters. As shown in Figure 4, six symmetry-related lead atoms (Pb1, Pb2, Pb3, Pb1A, Pb2A and Pb3A) were clustered by two $\mu_4\text{-O}^{2-}$ anions (O9 and O9A). Then, the cluster was edge-bridged by eight different carboxylate groups (O-C1-O, O-C1A-O, O-C5C-O, O-C5H-O, O-C13-O, O-C13A-O, O-C17B-O, and O-C17D-O) of the tip ligands to give an 8-connected centrosymmetric hexanuclear cluster SBU (secondary building unit) $\text{Pb}_6\text{O}_2(\text{COO})_8$. Each of the cluster SBUs was further interlinked by eight tip ligands, resulting in a 2D layer structure in *bc*

plane, as shown in Figure 5.

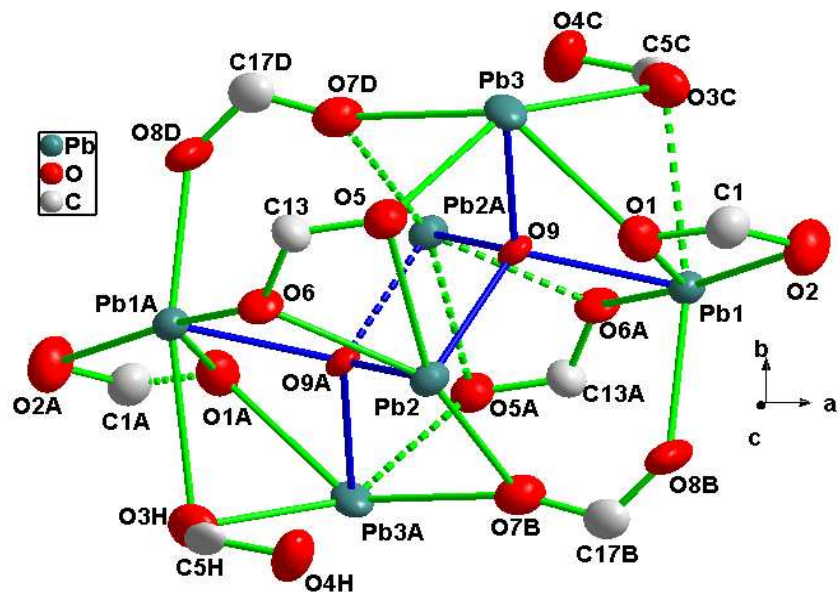


Figure 4 Schematic representation of an 8-connected hexanuclear cluster SBU $\text{Pb}_6\text{O}_2(\text{COO})_8$ for **2**. Symmetry codes: A (-x, 1-y, -z), B (-x, -0.5+y, 0.5-z), C (x, y, -1+z), D (x, 1.5-y, -0.5+z), H (-x, 1-y, 1-z)

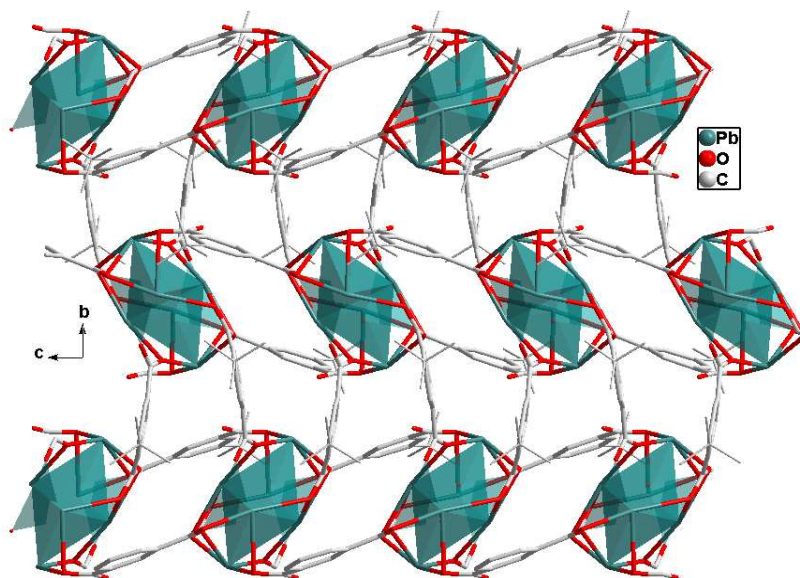


Figure 5 The 2D layer structure constructed from 8-connected Pb_6O_2 clusters and tip ligands for **2**. Hexanuclear clusters are represented in polyhedrons for clarity.

Topologically, the tip ligands could be viewed as the linkers, and each Pb_6O_2 cluster served for a 6-connected node. The equivalent 2D topology framework for **2** can be viewed as a uninodal **hxl**-type topological motif with a Schläfli symbol of $(3^6.4^6.5^3)$, as shown in Supporting Information

ESI 2.

Crystal structure of $[\text{Pb}_4(\mu_4\text{-O})(\text{tip})_3]_n$ (3**) :**

Compound **3** crystallized in the orthorhombic space group $Pna2_1$. The structure of **3** featured a complicated 3D network. The asymmetric unit of **3** contained four crystallographically unique Pb^{2+} ions, one $\mu_4\text{-O}^{2-}$ anion, and three tip anions. As shown in Figure 6, Pb1, Pb2, and Pb3 were all six-coordinated by five carboxylate oxygen atoms (O1, O5, O6, O12, and O3A belong to Pb1; O1, O2, O8C, O9C, and O4A belong to Pb2; O5, O11, O7C, O8C, and O10C belong to Pb3) from four different tip anions and one oxygen atom from $\mu_4\text{-O}^{2-}$ anion (O13). Pb4 adopted another kind of coordination manner. It coordinated with five carboxylate oxygen atoms (O10C, O11, O12, O3A, and O4A belong to Pb4A) from three different tip anions and one oxygen atom from $\mu_4\text{-O}^{2-}$ anion (O13). Distances of Pb–O in the range 2.283–2.818 Å were in good agreement with reported values.⁸ Only the Pb–O bond distances for Pb4A–O10C [2.883 Å], Pb4A–O11 [2.932 Å], and Pb2–O2 [2.938 Å], were longer, but the values were still in the bonding range.⁹ At the same time, the subtle distinction among Pb1, Pb2, Pb3 and Pb4 originated from three kinds of tip ligands adopting four, five, and six coordination numbers, respectively. The detailed coordination modes for these three tip ligands were described in Chart 1a, 1b, and 1d.

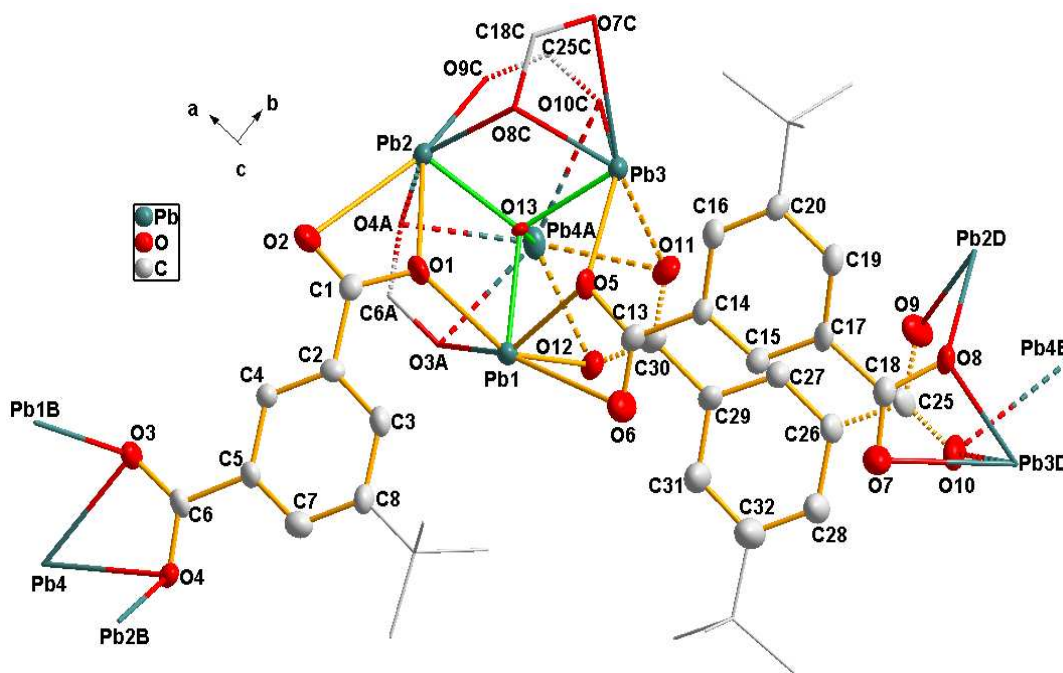


Figure 6 The coordination geometry of the tip ligand and Pb atoms in **3**. Hydrogen atoms are omitted for clarity. Symmetry codes: A (2-x, 1-y, 0.5+z), B (2-x, 1-y, -0.5+z), C (0.5+x, 1.5-y, z), D (-0.5+x, 1.5-y, z), E (1.5-x, 0.5+y, 0.5+z)

It is worth noting that one μ_4 -oxygen atom (O13) connected the four crystallographically unique Pb atoms into an isolated tetrahedral cluster Pb_4O , which further shared with the six carboxylate groups (O-C1-O, O-C13-O, O-C30-O, O-C6A-O, O-C18C-O, and O-C25C-O), resulting in a 6-connected tetranuclear cluster SBU (secondary building unit) $Pb_4O(COO)_6$, as shown in Figure 7. Each of the cluster SUBs was further linked to four neighboring ones by six tip ligands, reticulating into the final 3D porous framework (Figure 8). By virtue of the PLATON analysis,¹⁰ approximately 41.5% of the crystal volume is occupied by the bulky tertbutyl groups (1657.5 out of the 3991.1 Å³ in each cell unit), which means that the compound **3** has a microporous framework dwelt in the disordered tertbutyl groups.

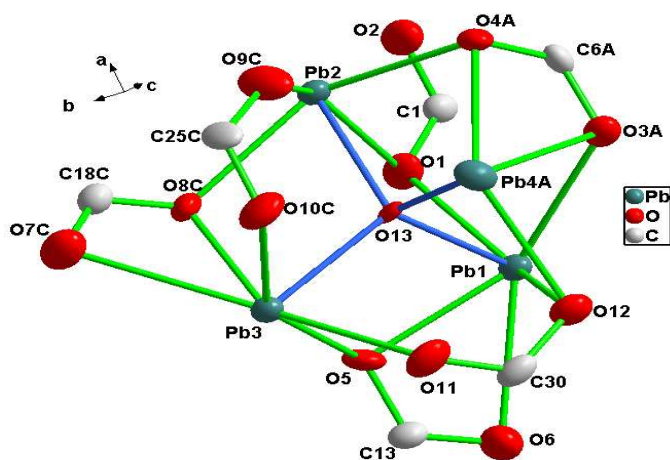


Figure 7 Schematic representation of a 6-connected tetranuclear cluster SBU $Pb_4O(COO)_6$ for **3**. Symmetry codes: A (2-x, 1-y, 0.5+z), C (0.5+x, 1.5-y, z)

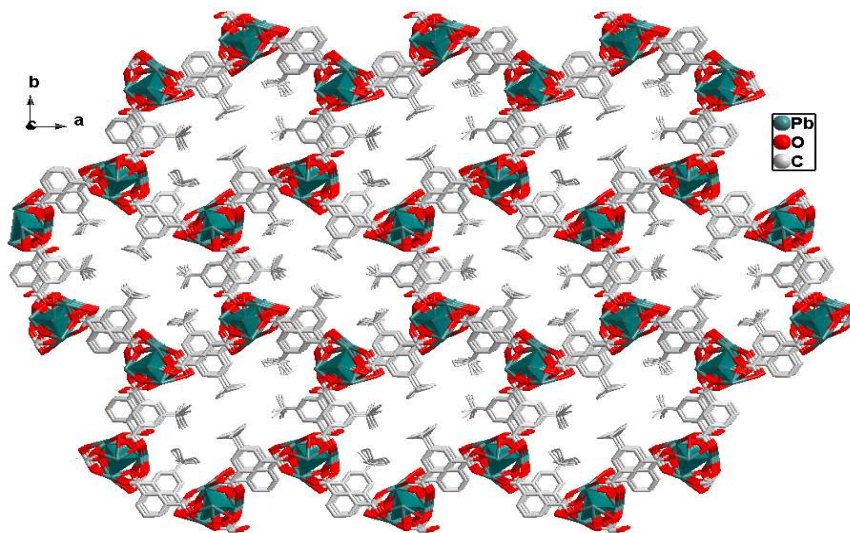


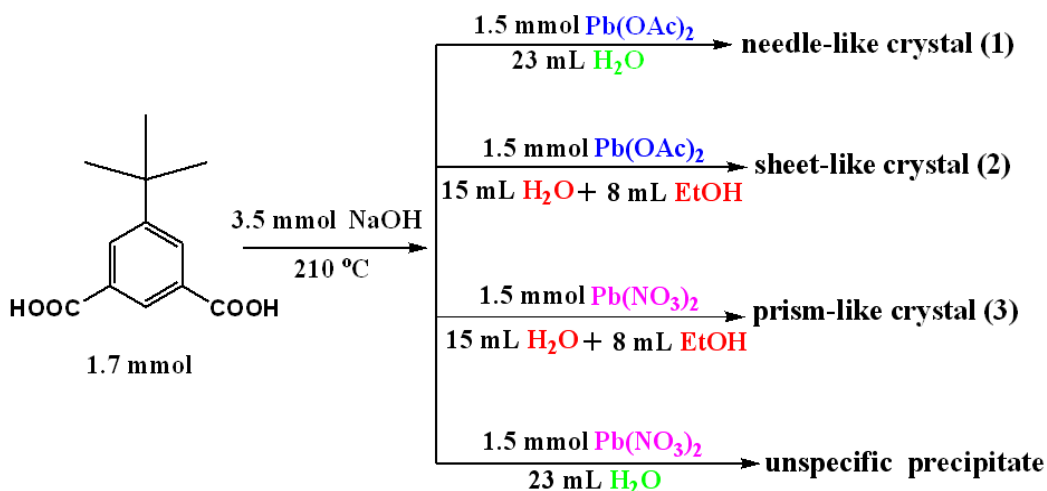
Figure 8 The 3D microporous framework constructed from 6-connected Pb_4O clusters and tip ligands for **3**. Tetranuclear clusters are represented in polyhedrons for clarity.

As shown in Supporting Information ESI 3, the tetrahedral Pb_4O clusters acted as 4-connected nodes and the tip groups acted as the linkers. The equivalent 3D topology framework for **3** could be viewed as a uninodal **dia**-type topological motif with a Schläfli symbol of (6^6) .

Solvent and counteranion-induced synthesis:

The basic consideration of our synthetic strategy was to study the influence of solvent and counteranion on the structures and photoluminescent properties of Pb-based MOFs with the ligand 5-tert-butylisophthalic acid. Under the similar reaction conditions, we selected the same amounts of 5-tert-butylisophthalic acid, NaOH, lead salts of nitrate and acetate, water and water/ethanol mixture as the starting materials to make this investigation. As shown in Chart 2, when 5-tert-butylisophthalic acid, NaOH, lead acetate were chosen as the reactants, use of solvent water alone generated the crystal product of $[\text{Pb}(\text{H}_2\text{O})(\text{tip})]_n$ (**1**), which presented a 2D bilayer structure.

Chart 2 Solvent and counteranion-induced synthesis



When the solvent was changed from pure water to water/ethanol mixture (15:8, V/V) with everything else kept the same as in **1**, the other crystal $[\text{Pb}_3(\mu_4\text{-O})(\text{tip})_2]_n$ (**2**) with a different 2D layer structure was formed. With the counteranion as the only variable, following the procedure adopted for **2**, changing the lead acetate to nitrate afforded crystal sample $[\text{Pb}_4(\mu_4\text{-O})(\text{tip})_3]_n$ (**3**) as a novel 3D porous framework. However, following the synthesis process of **3**, when the solvent mixture (water/ethanol) was substituted with the pure solvent (water), only unspecific white precipitates were obtained, which was perhaps due to the quick hydrolysis of lead nitrate under the pure solvent conditions. In contrast to **1**, no solvent was incorporated into **2** and **3**, which may be

likely due to the different solvent polarity or the configuration of solvent molecules. Furthermore, no nitrate or acetate ion was bonded to the lead center for the Pb-based MOFs mentioned above. At the same time, once isolated, all of the Pb-based MOFs were stable in air and insoluble in common organic solvents and water. From the chart 2, it is evident that MOFs **1** and **2** had selectivity for specific solvents during the synthetic process. And the selectivity for specific counteranions was also found in MOFs **2** and **3**. The above observations suggested both solvent and counteranion played crucial roles in controllable synthesis of MOFs under the same amounts of starting materials and similar reaction conditions. The water/ethanol mixture and counteranions (acetate) might be highly efficient as structure-directing agents during the reaction processes, since the coordination environment around the building units or metal centers was always affected by the excellent H-bond formation abilities of the water/ethanol mixture and acetate. The findings of the in situ solvent and counteranion-induced synthesis strategy afforded us new opportunities for the rapidly designing materials with interesting structures and properties.

FT-IR spectra, thermogravimetric analyses and PXRD patterns

The FT-IR spectra of **1**, **2** and **3** exhibited characteristic bands of the asymmetric stretching vibrations of the carboxylate groups at 1630-1520 cm^{-1} , and the symmetric stretching vibrations between 1310 and 1480 cm^{-1} , respectively (Supporting Information ESI 4). The results indicated the existence of a deprotonated carboxylate group coordinated to the metal ion, in agreement with the solid-state structures.

In order to examine the thermal stability of the three compounds, thermogravimetric analyses (TGA) were performed on single-phase polycrystalline samples of these materials (Supporting Information ESI 5). For **1**, the first weight loss of 3.5 % (calculated value 4.0 %) occurred in the temperature range 30-140 $^{\circ}\text{C}$, which was equivalent to the release of the coordinated water molecules. And then there was a plateau of stability before 360 $^{\circ}\text{C}$, indicating that the framework of **1** can be stable up to 360 $^{\circ}\text{C}$. Upon heating above 360 $^{\circ}\text{C}$, the rapid collapse of framework took place. This may be attributed to the decomposition of the ligand. **1** did not lose weight at higher temperature up to 550 $^{\circ}\text{C}$ and the residue (50.6 %, calculated value 50.1 %) might be PbO. For **2** and **3**, no weight loss was observed from room temperature to 380 $^{\circ}\text{C}$ in the TG curves, which indicated that both of them were anhydrous. Evidently, the TGA results for **2** and **3** were also in accordance with the single crystal structure analysis. From 380 to 580 $^{\circ}\text{C}$, weight losses of 59.2 % and 62.1 % should be ascribed to the decomposing of the organic frameworks for **2** and **3**,

respectively, which were both in good agreement with the calculated values (59.3 % for **2**, 62.0 % for **3**), considering the final product as PbO.

The powder X-ray diffraction patterns (PXRD) of **1**, **2** and **3** were performed in the room temperature (Supporting Information ESI 6). The different structures of them have also been indicated by their different XRPD patterns. Furthermore, all the XRPD patterns measured for the as-synthesized samples were all in good agreement with those simulated from single crystal structural data. Thus all the compounds **1**, **2** and **3** were obtained as a single phase, which proved the purity of the bulk phases.

Photoluminescent properties

With regard to MOFs, studies have been essentially restricted to d^{10} and 4f metals, and little attention has been paid to the luminescence of MOFs of main group metals such as Pb.^{1,2} It was noteworthy that the Pb(II) complexes were a potential class of functional materials with interesting photic properties, due to the fact that complexes of heavy metals with s^2 electron configuration might reduce the radiative lifetime of triplets by increasing spin-orbit coupling and promote emission from the triplet state under ambient conditions.¹¹ In this work, the photoluminescent properties of **1-3** have been explored in the solid state at room temperature. And in order to understand the nature of these emission bands, the photoluminescent properties of the free ligand were also examined. As shown in Figure 9, the free ligand H₂tip displayed the ultraviolet emission at 345 nm ($\lambda_{ex}=315$ nm), which could probably be assigned to the $\pi^* \rightarrow \pi$ transition.

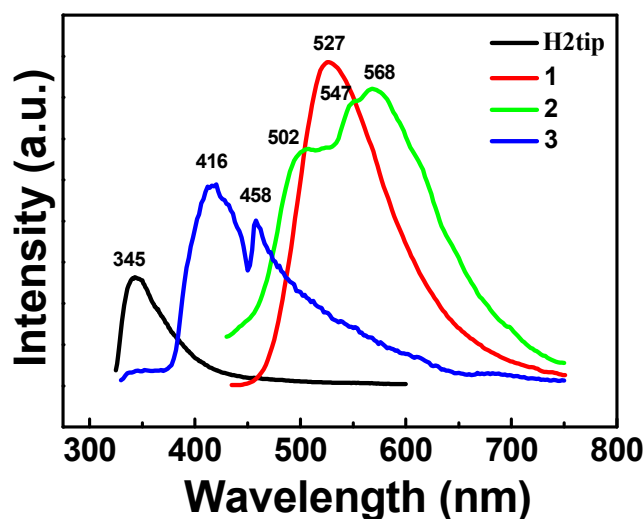


Figure 9 The emission spectra excited at 315, 360, 350 and 325 nm for H₂tip, **1**, **2** and **3**, respectively.

Three Pb-based MOFs displayed the emission bands centered at 527 nm ($\lambda_{\text{ex}}=360$ nm) for **1**, 502, 547 and 568 nm ($\lambda_{\text{ex}}=350$ nm) for **2**, 416 and 458 nm ($\lambda_{\text{ex}}=325$ nm) for **3**. It was evident that the emission bands of the Pb-based MOFs were all red-shifted compared to the free ligand, and emitted luminescence in the range 400-600 nm at room temperature. While the free ligand H₂tip exhibited no observable fluorescent emission in the range of 400-600 nm, which eliminated ligand-centered (LC) and ligand-to-ligand charge transfer (LLCT) excited states. Therefore, taking the emission bands of the free ligand into consideration, the emission bands at 416 and 458 nm of **3**, could be attributed to ligand-to-metal charge transfer (LMCT) between delocalized p bonds of the aromatic carboxylate groups and p orbitals of Pb(II) centers, which was similar to the reported literatures for the Pb-based MOFs.¹² Compared with **3**, the emission wavelengths of **1** and **2** became longer and should be different from that of LMCT. The low-energy emissions with large Stokes shifts, including 527 nm for **1**, 502, 547 and 568 nm for **2** could be assigned to metal-centered s→p transition as proposed by Vogler.¹³ These photoluminescent results implied that the coordination modes of Pb(II) cations played an important role in influencing the emissive peak position of compounds, and had significant influence on the emission mechanism of the Pb-based MOFs.

Conclusion

With solvents or counteranions as the only variable, hydrothermal reactions with the same amounts of 5-tert-butylisophthalic acid, NaOH, Pb(OAc)₂·3H₂O or Pb(NO₃)₂, afforded three new Pb-based metal-organic frameworks [Pb(H₂O)(tip)]_n (**1**), [Pb₃(μ₄-O)(tip)₂]_n (**2**) and [Pb₄(μ₄-O)(tip)₃]_n (**3**) under the same reaction conditions. Considering the synthetic process, the Pb-based compounds had selectivity for specific solvent and counterions in the self-assembly process. In this study, the water/ethanol mixture, nitrate and acetate ions could be highly efficient as structure-directing agents during the synthesis processes of Pb-based compounds. The structural analysis indicated that **1** featured a 2D bilayer structure containing a uninodal **sql**-type topological motif; The 2D layer framework of **2** was constructed from a unique 8-connected hexanuclear cluster secondary building unit Pb₆O₂(COO)₈, with a uninodal **hxl**-type topological motif. The 3D microporous framework of **3** was formed by a 6-connected tetranuclear cluster Pb₄O(COO)₆ with a uninodal **dia**-type topological motif. Furthermore, strong luminescent emissions are observed for **1**, **2** and **3**, which might be good candidates for photoluminescence materials. Considering the fact that Pb-based metal-organic frameworks **1**, **2** and **3** obtained under the same amounts of starting

materials and similar synthetic procedures, were distinct from each other, such as composition, topology, and photoluminescent properties, which could afforded us new opportunities for the rapidly designing materials with interesting structures and properties. The feasible strategy for controlling the synthesis of other framework architectures through this in situ solvent and counteranion-induced synthesis method were underway in our laboratory.

Experimental Section

Reagents and Instrumentation: Reagents were purchased commercially and were used without further purification. Elemental analyses (C and H), IR spectra, TG analyses, single crystal X-ray diffraction data, PXRD, solid-state emission and excitation spectra were all performed on the corresponding instruments similar with our recently published paper.⁴ And the crystal structures were solved by direction method and refined by a full matrix least-squares technique based on F^2 using SHELXL 97 program.¹⁴ All of the non-hydrogen atoms were refined anisotropically. The organic hydrogen atoms were generated geometrically, the aqua hydrogen atoms were located from difference maps and refined with isotropic temperature factors. Crystallographic data for the structures reported in this paper have been deposited with the Cambridge Crystallographic Data Centre as supplementary publication no. CCDC-1019800 (**1**), CCDC-1019801 (**2**) and CCDC-1019802 (**3**). Copies of the data can be obtained free of charge on application to CCDC, 12 Union Road, Cambridge CB21EZ, UK (fax: (+44) 1223-336-033; e-mail: deposit@ccdc.cam.ac.uk). The crystallographic data and structure refinement for all the MOFs were summarized in Table 1 .

Table 1 Crystal data and refinement parameters for **1**, **2** and **3**.

| Compound | 1 | 2 | 3 |
|---|---|--|---|
| Empirical formula | C ₁₂ H ₁₄ O ₅ Pb | C ₂₄ H ₂₄ O ₉ Pb ₃ | C ₃₆ H ₃₆ O ₁₃ Pb ₄ |
| Formula weight | 445.42 | 1078.00 | 1505.41 |
| Crystal system | Orthorhombic | Monoclinic | Orthorhombic |
| Space group | <i>Iba</i> 2 | <i>P</i> 2 ₁ / <i>c</i> | <i>Pna</i> 2 ₁ |
| <i>a</i> / Å | 16.2354(8) | 18.7933(9) | 18.4043(5) |
| <i>b</i> / Å | 19.1181(10) | 17.7755(6) | 30.9956(9) |
| <i>c</i> / Å | 8.2268(4) | 8.2471(3) | 6.9963(2) |
| <i>α</i> / deg | 90 | 90 | 90 |
| <i>β</i> / deg | 90 | 99.723(4) | 90 |
| <i>γ</i> / deg | 90 | 90 | 90 |
| Volume/ Å ³ | 2553.5(2) | 2715.46(19) | 3991.1(2) |
| <i>Z</i> | 8 | 4 | 4 |
| ρ_{cal} /g·cm ⁻³ | 2.317 | 2.637 | 2.505 |
| μ /mm ⁻¹ | 13.224 | 18.602 | 16.884 |
| <i>F</i> (000) | 1664 | 1944 | 2736 |
| GOF | 1.023 | 1.029 | 1.055 |
| <i>R</i> ₁ (<i>I</i> >2 σ (<i>I</i>)) | 0.0326 | 0.0599 | 0.0354 |
| <i>wR</i> ₂ (<i>I</i> >2 σ (<i>I</i>)) | 0.0678 | 0.1319 | 0.0749 |
| <i>R</i> ₁ (all data) | 0.0557 | 0.0975 | 0.0410 |
| <i>wR</i> ₂ (all data) | 0.0799 | 0.1551 | 0.0778 |
| Flack parameter | 0.07(3) | | 0.038(13) |

Preparation of MOFs

Synthesis of **1**: A mixture of 1.5 mmol Pb(OAc)₂·3H₂O, 1.7 mmol 5-tert-butylisophthalic acid (H₂tip), and 3.5 mmol NaOH in 23mL H₂O, was stirred for 20 min at room temperature (the pH value of the mixture was 7). The mixture was then heated in a Teflon-lined stainless steel autoclave (40 ml) at 210 °C for 4 days under static conditions. After cooling the reaction mixture to room temperature, white needle-like crystals were separated and washed by distilled water many times. Finally, the products were dried in air at room temperature (Yields: ~ 75%).

Elemental analysis (%) calcd for **1**: C 32.36, H 3.17; Found: C 32.29, H 3.22

IR (KBr, cm⁻¹) for **1**: 3615 w, 3299 m, 3175 w, 2965 s, 2910 w, 2866 w, 1628 w, 1609 w, 1598 s, 1518 s, 1430 m, 1370 m, 1356 m, 1312 m, 1273 m, 1205 w, 1180 m, 1130 w, 1114 m, 927 w, 910 m, 822 s, 787 s, 754 s, 726 s, 696 m, 602 w, 578 w, 520 w, 481 w

Synthesis of **2**: A mixture of 1.5 mmol Pb(OAc)₂·3H₂O, 1.7 mmol 5-tert-butylisophthalic acid

(H₂tip), and 3.5 mmol NaOH in 15mL H₂O and 8 mL alcohol dehydrated, was stirred for 20 min at room temperature (the pH value of the mixture was 7). The mixture was then heated in a Teflon-lined stainless steel autoclave (40 ml) at 210°C for 4 days under static conditions. After cooling the reaction mixture to room temperature, white sheet-like crystals were separated and washed by distilled water many times. Finally, the products were dried in air at room temperature (Yields: ~ 70%).

Elemental analysis (%) calcd for **2**: C 26.74, H 2.24; Found: C 26.65, H 2.16

IR (KBr, cm⁻¹) for **2**: 3422 s, 2965 s, 2910 w, 2873 w, 1846 w, 1603 s, 1540 s, 1480 m, 1433 s, 1400 m, 1370 s, 1350 s, 1312 w, 1268 s, 1204 w, 1177 w, 1114 s, 1045 w, 1001 w, 927 m, 907 m, 820 s, 781 s, 751 s, 721 s, 696 w, 608 w, 578 w, 514 w, 484 w

Synthesis of **3**: Synthesis of **3** was similar to that of **2** using Pb(NO₃)₂ instead of Pb(OAc)₂·3H₂O (the pH value of the mixture was 7). White prism-shaped crystals of **3** were obtained (Yields: ~ 80%).

Elemental analysis (%) calcd for **3**: C 28.72, H 2.41; Found: C 28.68, H 2.38

IR (KBr, cm⁻¹) for **3**: 3435 s, 2959 s, 2873 w, 1851 w, 1631 s, 1595 s, 1548 w, 1513 s, 1480 w, 1463 w, 1425 m, 1367 m, 1351 s, 1309 s, 1279 s, 1254 m, 1205 w, 1161 m, 1130 w, 1111 w, 1004 w, 910 m, 814 m, 776 s, 754 m, 721 s, 713 s, 600 w, 578 w, 512 w, 487 w

Acknowledgements

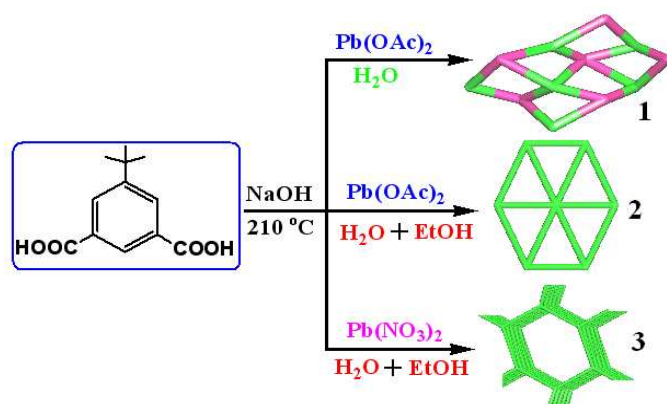
We gratefully acknowledge financial support by the National Natural Science Foundation of China (grant no. 21171068) and the Shandong Provincial Natural Science Foundation of China (grant no. ZR2010BM036, ZR2013BQ009).

Reference

- (a) H. Furukawa, K.E. Cordova, M. O'Keeffe and O.M. Yaghi, *Science*, 2013, **341**, 1230444; (b) W. Lu, Z. Wei, Z.Y. Gu, T.F. Liu, J. Park, J. Park, J. Tian, M. Zhang, Q. Zhang, T. GentleIII, M. Bosch and H.C. Zhou, *Chem. Soc. Rev.*, 2014, **43**, 5561; (c) J. Liu, L. Chen, H. Cui, J. Zhang, L. Zhang and C.Y. Su, *Chem. Soc. Rev.*, 2014, **43**, 6011; (d) J.B. Decoste, G.W. Peterson, *Chem. Rev.*, 2014, **114**, 5695; (e) C. Wang, D. Liu and W. Lin, *J. Am. Chem. Soc.*, 2013, **135**, 13222.
- (a) A. Santra and P.K. Bharadwaj, *Cryst. Growth Des.*, 2014, **14**, 1476; (b) X.M. Lin, T.T. Li, L.F. Chen, L. Zhang and C.Y. Su, *Dalton Trans.*, 2012, **41**,10422; (c) S.C. Chen, Z.H. Zhang, Y.S.

- Zhou, W.Y. Zhou, Y.Z. Li, M.Y. He, Q.Chen and M. Du, *Cryst. Growth Des.*, 2011, **11**, 4190.
- 3 (a) A.P. Neal and T.R. Guilarte, *Toxicol. Res.*, 2013, **2**, 99; (b) C.V. Gherasim, J. Křivčík and P. Mikulášek, *Chem. Eng. J.*, 2014, **256**, 324; (c) M.S. Tellis, M.M. Lauer, S. Nadella, A. Bianchini and C.M. Wood, *Aquat. Toxicol.*, 2014, **146**, 220; (d) A. Üstünda, C. Behm, W. Föllmann, Y. Duydu and G.H. Degen, *Arch. Toxicol.*, 2014, **88**, 1281.
- 4 (a) Q.B. Bo, H.Y. Wang, D.Q. Wang, Z.W. Zhang, J.L. Miao and G.X. Sun, *Inorg. Chem.*, 2011, **50**, 10163; (b) Q.B. Bo, H.Y. Wang, J.L. Miao and D.Q. Wang, *RSC Advances*, 2012, **2**, 11650; (c) Q.B. Bo, H.Y. Wang and D.Q. Wang, *New J. Chem.*, 2013, **37**, 380; (d) Q.B. Bo, H.T. Zhang, H.Y. Wang, J.L. Miao and Z.W. Zhang, *Chem. Eur. J.*, 2014, **20**, 3712.
- 5 (a) Q.B. Bo, Z.X. Suna and W. Forsling, *CrystEngComm*, 2008, **10**, 232 ; (b) X. Liu, P. Cen, H. Li, H. Ke, S. Zhang, Q. Wei, G. Xie, S. Chen and S. Gao, *Inorg. Chem.*, 2014, **53**, 8088; (c) L.L. Qu, Y.L. Zhu, Y.Z. Li, H.B. Du and X.Z. You, *Cryst. Growth Des.*, 2011, **11**, 2444; (d) J. Qian, J. Hu, J. Zhang, H. Yoshikawa, K. Awaga and C. Zhang, *Cryst. Growth Des.*, 2013, **13**, 5211; (e) J. Li, S. Meng, J. Zhang, Y. Song, Z. Huang, H. Zhao, H. Wei, W. Huang, M.P. Cifuentes, M.G. Humphreyd and C. Zhang, *CrystEngComm*, 2012, **14**, 2787.
- 6 (a) H.T. Xiao and A. Morsali, *Solid State Sci.*, 2007, **9**, 155; (b) J. L. Song, C. Lei, Y.Q. Sun, J.G. Mao, *J. Solid State Chem.*, 2004, **177**, 2557; (c) J.L. Song, J.G. Mao, Y.Q. Sun and A. Clearfield, *Eur. J. Inorg. Chem.*, 2003, 4218; (d) M.R.St.J. Foreman, T. Gelbrich, M.B. Hursthouse and M.J. Plater, *Inorg. Chem. Commun.*, 2000, **3**, 234.
- 7 (a) X. Zhang, J.K. Cheng, F. Chen, M.L. Sun and Y.G. Yao, *Inorg. Chem. Commun.*, 2011, **14**, 358; (b) K.L. Zhang, Y. Chang, C.T. Hou, G.W. Diao, R.T. Wu, S.W. Ng, *CrystEngComm*, 2010, **12**, 1194; (c) X.L. Wang, Y.Q. Chen, Q. Gao, H.Y. Lin, G.C. Liu, J.X. Zhang and A.X. Tian, *Cryst. Growth Des.*, 2010, **10**, 2174; (d) J. Yang, J.F. Ma, Y.Y. Liu, J.C. Ma and S.R. Batten, *Cryst. Growth Des.*, 2009, **9**, 1894.
- 8 (a) R. Abhinandan, K.J. Swapan, B. Madhusudan, H. Debdoot, S.C. Durga, Z. Ennio and D. Sudipta, *J. Solid State Chem.* 2013, **197**, 46; (b) J.D. Lin, S.T. Wu, Z.H. Li and S.W. Du, *CrystEngComm*, 2010, **12**, 4252; (c) L. Zhang, Z.J. Li, Q.P. Lin, Y.Y. Qin, J. Zhang, P.X. Yin, J.K. Cheng and Y.G. Yao, *Inorg. Chem.*, 2009, **48**, 6517.
- 9 (a) X.H. Lou, C. Xu, H.M. Li, Z.Q. Wang, H. Guo, D.X. Xue, *CrystEngComm*, 2013, **15**, 4606; (b) D. Sunirban, K. Hyunuk and K. Kimoon, *J. Am. Chem. Soc.*, 2009, **131**, 3814; (c) P. Du, Y. Yang, J. Yang, Y.Y. Liu, W.Q. Kan and J.F. Ma, *CrystEngComm*, 2013, **15**, 6986.

- 10 A. L. Spek, *PLATON 99, A Multipurpose Crystallographic Tool*, Utrecht University, Utrecht, The Netherlands, 1999.
- 11 S. K. Dutta and M. W. Perkovic, *Inorg. Chem.*, 2002, **41**, 6938.
- 12 (a) E.C. Yang, J. Li, B. Ding, Q.Q. Liang, X.G. Wang and X.J. Zhao, *CrystEngComm*, 2008, **10**, 158; (b) X.Q. Li, H.B. Zhang, S.T. Wu, J.D. Lin, P. Lin, Z.H. Li and S.W. Du, *CrystEngComm*, 2012, **14**, 936.
- 13 (a) P. C. Ford and A. Vogler, *Acc. Chem. Res.*, 1993, **26**, 220; (b) A. Vogler, A. Paukner and H. Kunkely, *Coord. Chem. Rev.*, 1980, **33**, 227; (c) H. Nikol, A. Becht and A. Vogler, *Inorg. Chem.*, 1992, **31**, 3277; (d) G. Blasse and B. C. Grabmaier, *Luminescent Materials*, Springer Verlag: Berlin, 1994.
- 14 (a) G.M. Sheldrick, *SHELXL-97*, University of Göttingen: Göttingen, Germany, 1997; (b) G.M. Sheldrick, *Acta Crystallogr. Sect. A*, 2008, **64**, 112.



With solvents or counteranions as the only variable, three novel photoluminescent Pb-based metal-organic frameworks obtained under the similar synthetic procedures.